



Fresh mechanical and durability properties of alkali-activated fly ash-slag concrete: a review

H. S. Abhishek¹ · Shreelaxmi Prashant¹ · Muralidhar V. Kamath¹ · Mithesh Kumar¹

Received: 16 September 2021 / Accepted: 15 November 2021 / Published online: 1 December 2021
© The Author(s) 2021

Abstract

This paper describes a review of the state-of-the-art research carried on the fresh and hardened properties of Alkali Activated Binders and Concretes. Though, many research have been carried out in the recent times on alkali activated binders, few key parameters still remain unattended, that restricts the commercial application of AAMs to the general construction activities. Fresh properties, mechanical strength and durability performance of Alkali activated concrete with various Alumino silicates as base materials is mentioned. An essential parameter of Alkali activated concrete is the concentration of alkaline solution on which various properties like mechanical strength, setting time and durability depends. Influence of wide range of concentrations from 6 to 16 M on these properties are studied and reported in this paper. This paper mainly concentrates on properties of readily available base materials such as Fly ash and Slag and the means to improve their performance through the use of various industrial and agro-based byproducts as additives. Problems pertaining to practical applicability of AAMs to general construction activities are also highlighted.

Keywords Fly ash · GGBFS · Alkali activated binders · Alkali activated concrete · Mechanical properties

Abbreviation

AAB	Alkali Activating Binders
AAC	Alkali Activated Concrete
AAFC	Alkali Activated Fly ash Concrete
AASC	Alkali Activated Slag Concrete
AAFSC	Alkali Activated Fly ash and Slag Concrete
CS	Compressive Strength
GGBFS	Ground Granulated Blast Furnace Slag
OPC	Ordinary Portland Cement

Introduction

Rapid advancement in infrastructure has resulted into ever increasing demand for Portland cement across the world. For every ton of cement production, a ton of carbon-di-oxide is released into the atmosphere, which ultimately accounts for 7% of global carbon-di-oxide emissions globally [1–3]. Depletion of natural resources, is yet another environmental

issue faced by the present generation researchers, has provoked the concrete technologists to look for an alternative to very popular Portland cement. Uncontrolled disposal of industrial by-products and agricultural wastes in the landfills has become yet another serious concern to the environment [4–6]. These issues together has led to the development of Alkali Activated materials in the recent years. This has proved to be a promising new generation material for concrete and similar applications since it consumes huge portions of industrial and agro wastes containing considerable proportions of alumino silicates. Most Popular among them is fly ash. The production of fly ash has been increased gradually in the past few decades globally. In the year 2018–2019 estimated around 217.04 million tons in India. 77.59% of the fly ash available globally is generated in India. Because of its availability fly ash finds its use in the cement industry, mine filling, bricks, and many other related applications [7–9].

AAC is an alternative technique to lower the consumption of cement in the concrete making. AAC is kind of concrete which is manufactured by aluminosilicates and alkaline solution. the binder so produced has setting and hardening properties similar to that of Portland Cement [10–12]. The reaction mechanism of alkali-activated concrete varies compared to that of Ordinary Portland Cement concrete compositions. The Reaction mechanism mainly depends on the composition of the aluminosilicates used. Therefore,

✉ Shreelaxmi Prashant
shreelaxmi.p@manipal.edu

¹ Department of Civil Engineering, Manipal Institute of Technology, Manipal Academy of Higher Education, Manipal, India

reaction mechanism of AAC can be classified (on the basis of their composition) into high calcium contents and low calcium alkali activation. In high calcium binders, the principal product formed as a binder is Calcium-Aluminum-Silicate-Hydrate gel. It forms a dense matrix exhibiting excellent engineering properties. The main products formed in a low calcium system are sodium-aluminosilicate-hydrate gels with pseudo-zeolite structures [11, 13–15].

Most popular aluminosilicates available are ground granulated blast furnace slag, fly ash, metakaolin, palm oil fuel ash, and rice husk ash etc. However, only categorizing the available literature on alkali activated binders, it is found that most of the studies are based on fly ash and GGBFS or a combination principally containing fly ash and GGBS. Alkali activators play an essential role in dissolution of atoms to form geopolymer precursors. Potassium Hydroxide, Sodium Hydroxide, Potassium Silicate, and Sodium Silicate are alkaline solutions that have been used popularly [16–19]. Commonly used alkaline liquids are Sodium Hydroxide and Sodium Silicate. Alkali activated aluminosilicates materials have a considerably lower carbon footprint in comparison with Ordinary Portland cement, exhibiting enhanced strength and chemical resistance properties [20–22]. The representation of the synthesis of alkali-activated material (Fig. 1).

The study of short-term and long-term properties of AAC is still unexplored. The advantages of alkali-activated concrete are utilizing agricultural waste materials and industrial by-products to manufacture concrete and since it consumes a lot of by products, it proves environmentally friendly. The properties influencing the fresh properties are studies from the available literature. The fresh properties of the binder system are reported in terms of mini-slump flow of paste and setting time. The oxides composition of various industrial and agro binders are discussed since they largely influence

the mechanical properties of AAC. The paper also reports the details of various alkaline solutions used by researchers and their influence on fresh and hardened properties of AAC.

Historical background of AAC

The technology of slag cement predates by more than a century, with a patent awarded to Kuhl [23] in 1908 and later in 1930, wherein slag was activated with alkaline liquid comprising of potassium hydroxide. In 1937, Chassevent [24] conducted experimental research on the reactivity of slag by using an alkaline solution consisting of potassium hydroxide and sodium hydroxide. Purdon [25] proposed mixing slag and dry solid sodium hydroxide and then adding water to prepare a mortar mixture in 1940.

Glushkovsky [26] successfully attempted preparing binder compositions based on accessible calcium-aluminosilicate sources using alkaline liquid in 1959. Later in 1979, the term “geopolymer” was coined by Davidovits [27]. In 1985, Davidovits and Sawyer [28] studied early high-strength mineral polymer composition using strong alkalis such as water, potassium hydroxide, sodium hydroxide, potassium poly-silicate, and sodium poly-silicate solutions. Sodium silicate and small amounts of hydrated lime were used as an alkali solution to develop alkali-activated slag concrete by Douglas et al. [29] in 1991. Wang and Scrivener [30] researched the microstructure development of alkaline activation of slag pastes in 1995. The mechanism of activation of fly ash with alkali-activated solutions was described by Palomo et al. [31] in 1999. Later, in 2006 Fernandez-Jimenez et al. [32] studied engineering properties such as



Fig. 1 Representation of synthesis of alkali-activated materials [81]

mechanical properties, modulus of elasticity, bond strength, and shrinkage of alkali-activated concrete.

Behavior steel corrosion in carbonated alkali-activated slag concrete was studied by Aperador et al. [33] in 2009. In 2012, Chi [34] conducted experimental research on the durability of AASC and the effect of dosage. Recently, Machine learning has been used by various authors to study the properties of AAC. Gomaa et al. [35] used machine learning to predict fresh and mechanical properties of AAC in 2020.

Materials

Aluminosilicate materials

Industrial by-products such as Ground Granulated Blast Furnace Slag, fly ash, and agricultural waste such as palm oil fuel ash, rice husk ash, and sugarcane bagasse ash are familiar sources of aluminosilicate materials used for alkali-activated binders [36]. The main compositions of these materials are alumina, magnesium, calcium, iron, and silica, which promote the reactivity mechanism in the AAB system. The Cementitious alkali-activated system components are shown in Fig. 2.

Fly ash

Fly ash is a by-product of the pulverized coal from thermal power plants. Fly ash is classified into two types, i.e., Class C and Class F [37]. Class C is a high calcium fly ash that contains more than 20% lime, and Class F is a low calcium fly ash with less than 7% lime. Class F fly ash is the best aluminosilicate source to be used as a base material because of its spherical structure, highly reactive phase, lower price, and abundance [38]. Class C fly ash is used less frequently

for manufacturing alkali-activated concrete due to its rapid setting [39] and not as readily available as Class F [40, 41].

Ground granulated blast furnace slag

GGBFS is a by-product of iron and steel manufacturing from the blast furnace, and then it is passed through water. The produced granular product is dried, and then it is ground into a powder. GGBFS is high in Calcium-Silicate-Hydrates and highly cementitious, a strength-enhancing compound that improves the mechanical properties of the concrete. GGBFS is commonly mixed with fly ash (Class F) to improve the reaction mechanism of the AAC [13]. GGBFS alone can be used in AAC, but the major drawback is that high calcium content in GGBFS accelerates the reaction of alkaline binders leads to early setting time [38, 42].

Oxide composition of fly ash and GGBFS

Since Fly ash and GGBFS is industrial by products, their compositions vary from depending on the process they have undergone. The performance of Alkali activated binders depend on the oxide compositions of the base materials. The oxide composition of fly ash and GGBFS using X-Ray Fluorescence is shown in Table 1. Fly ash and GGBFS possess a large amount of alumina, calcium, and silica. The chemical constituents of Class F fly ash reported in the literature referred for this study, here mainly comprises silicon-di-oxide (SiO₂) and aluminum oxide (Al₂O₃), Class C fly ash primarily includes Silicon-di-oxide (SiO₂), aluminum oxide (Al₂O₃), and calcium oxide (CaO). GGBFS comprises silica oxide (SiO₂) and calcium oxide (CaO) as a significant constituent. The

Fig. 2 Cementitious alkali-activated system components [44]

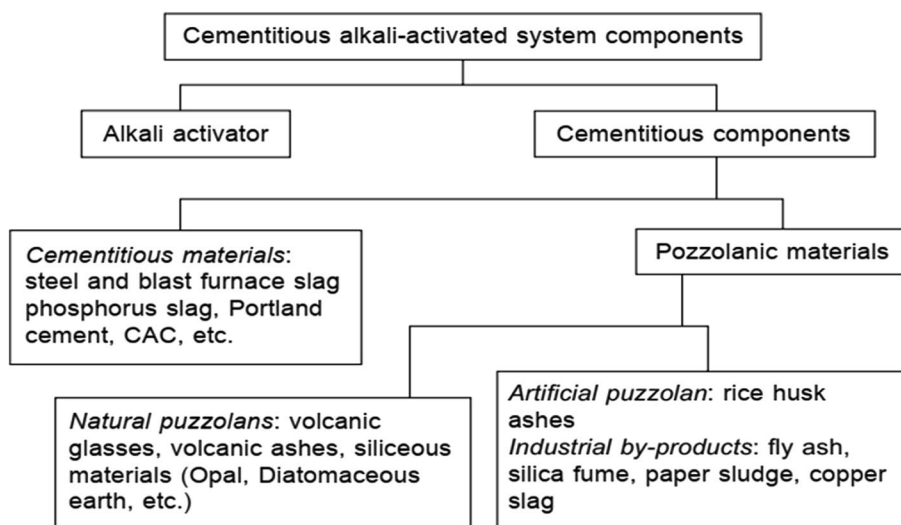


Table 1 Oxide Composition of fly ash and GGBF

	SiO ₂	Al ₂ O ₃	Fe ₂ O ₃	CaO	MgO	SO ₃	SO ₄	K ₂ O	S	Na ₂ O	MnO	TiO ₂	P ₂ O ₅	LOI	Authors
FA	53.09	24.8	8.01	2.44	1.94	0.23	-	3.78	-	0.73	-	-	-	3.59	Fernandez-Jimenez et al. [32]
(Class F)	50.5	26.57	13.77	2.13	1.54	0.41	-	0.77	-	0.45	-	-	1	0.6	Sarker et al. [67]
	46	33	10.5	2.6	-	-	-	-	-	-	-	-	-	-	Lee and Lee [82]
	50	28.25	13.5	1.79	0.89	0.38	-	0.46	-	0.32	-	1.54	0.98	0.64	Nath and Sarker [52]
	50.7	28.8	8.8	2.38	1.39	-	-	2.4	-	0.84	-	-	-	3.79	Okoye et al. [61]
	70.3	23.1	1.4	0.2	0.6	0.2	-	0.9	-	0.4	-	2.6	0.2	2	A. Wardhono et al. [66]
	56.8	23.8	7.2	4.8	1.5	-	-	1.6	0.3	0.8	-	1.2	0.51	1.2	Nedeljković et al. [38]
	53.24	26.42	1.65	3.65	9.55	0.56	-	2.57	-	0.76	-	0.86	-	-	Fang et al. [54]
	64.97	26.64	5.69	0.33	0.85	-	0.33	0.25	-	0.49	-	-	-	0.45	Adak and Mandal [70]
	53.59	28.46	8.71	4.23	1.84	0.96	-	1.63	-	0.58	-	-	-	-	Mehta et al. [14]
	60.42	31.06	3.34	0.93	0.46	0.1	-	0.95	-	-	0.03	2.02	0.41	-	Dineshkumar and Umarani [53]
FA	38.7	20	15.3	16.6	1.5	2.6	-	2.7	-	1.2	-	0.4	0.1	0.1	Chindaprasirt et al.[49]
(Class C)	37.7	20	5.6	23.4	4.3	2.4	-	0.6	-	1.7	-	-	-	-	Thomas and Peethamparan [60]
	50.16	15.57	9.61	17.6	0.9	1.63	-	1.86	-	-	-	1.93	-	-	J. Stolz et al. [83]
GGBFS	21	17	0.62	56.1	-	0.77	-	-	-	-	-	-	-	-	Lee and Lee [82]
	32.46	14.3	0.61	43.1	3.94	4.58	-	0.33	-	0.24	-	0.55	0.02	0.09	Nath and Sarker [52]
	36.9	14.2	0.3	36	5.1	6.1	-	0.1	-	-	0.4	0.6	0.4	0.3	A. Wardhono et al. [66]
	35.5	13.5	0.64	39.8	8	-	-	0.53	1	0.4	-	1	-	-1.3	Nedeljković et al. [38]
	36.77	13.56	0.41	37.6	7.45	1.82	-	0.55	-	0.25	-	0.79	-	-	Fang et al. [54]
	33.86	20.4	0.8	33.67	7.89	0.9	-	-	-	0.12	-	-	-	0.36	Thunuguntla and Rao [56]
	35.8	13.21	1.97	35.68	9.76	0.21	-	0.57	-	0.48	-	-	-	-	Mehta et al. [14]
	34.42	16.62	0.64	38.27	5.99	1.57	-	0.31	-	-	1.04	0.84	-	-	Dineshkumar and Umarani [53]

oxide composition of fly ash and GGBFS used by various authors are shown in Table 1.

Alkaline activator solution

Potassium silicate (K₂SiO₃), potassium hydroxide (KOH), sodium silicate (Na₂SiO₃), and sodium hydroxide (NaOH) are used as alkaline solutions. In most of the studies either NaOH or Na₂SiO₃ solutions or a combination of both are used primarily used as activators. Few studies have reported the use of KOH and K₂SiO₃ in the similar lines [16]. The alkaline liquids dissolve the silica and aluminum atoms present in the aluminosilicate to form silicon-oxygen-aluminum (Si–O–Al) bonds as the polymerization process [43]. Though Potassium hydroxide is more alkaline than sodium hydroxide, the dissolution rate of silica and alumina in sodium hydroxide solution is found to be higher [36]. The polymerization process is rapid if sodium or potassium silicates are used with alkaline hydroxide as compared to use of only hydroxides of sodium or potassium. Sodium hydroxide is obtained from Brine electrolysis, and they are available in three forms, i.e., flakes, beads, and solids. Flakes are manufactured by feeding molten sodium hydroxide through cooled flaking rolls. Beads are obtained by passing molten solution into the prilling tower. Solids are produced by cooling molten caustic soda. The particle sizes of flakes, beads,

and solids are different, whereas the chemical composition is the same. Sodium silicate is obtained from carbonate salts and silica by calcination and adding the required amount of water [44]. concentration of NaOH used for preparing AAC depends on the performance level expected. Higher concentration which accelerates the reaction of raw materials. The sodium carbonate (Na₂CO₃) is also an alkaline solution, that can be used for GGBFS based AAB [45]. Influence of variation of molarity of NaOH and ratio of NaOH to Na₂SiO₃ as reported by the various researchers is shown in Table 2.

Fresh properties of AAB

Mini-slump flow of paste

The mini-slump cone test is used to measure the fluidity of fresh paste [46]. Nedeljkovic et al. [38] conducted a series of experiments for the flow test using a mini-slump cone with varying percentages of slag and with various alkaline liquid to binder ratio. With decrease in fly ash content, the spread diameter gradually decreased as the proportion of slag increased from 0 to 100%... The smooth glassy surface and spherical shape of fly ash particles promoted the sliding of the particles which increased the fluidity of paste Alkaline solution to binder ratio has been used from 0.3 to 0.7 in

Table 2 Molarity of NaOH and ratios of NaOH to Na₂SiO₃

Authors	Molarity of NaOH	Ratio of NaOH to Na ₂ SiO ₃
Somna et al. [58]	4.5, 7.0, 9.5, 12.0, 14.0 and 16.5	-
Sarker [59]	14	1:2.5
Sarker et al. [67]	14	1:1.5
Lee and Lee [82]	4, 6 and 8	1:0.5, 1:1 and 1:1.5
Nath and Sarker [52]	14	1:1.5, 1:2 and 1:2.5
Okoye et al. [61]	14	1:2.5
Adak et al. [84]	12	1:1.8
Wardhono et al. [66]	10 and 15	1:2
Mohankumar and Manickavasagam [85]	8, 10, 12 and 14	1:2.5
Duan et al. [86]	10	1:1.5
Thunuguntla and Rao [56]	1 and 8	1:1.5
Fang et al. [54]	10 and 12	1:1.5, 1:2 and 1:2.5
Stolz et al. [83]	8	-
Sakulich et al. [87]	8	1:2
Adak and Mandal [70]	8	1:1.8
Mehta et al. [14]	5–20	1:2 to 1:2.75
Sevinc and Durgun [88]	10, 12, 14	1:0.75 and 1:1.5
Das et al. [89]	12	1:2

the previous research. Most of the studies used solution to binder ration ranging from 0.4 to 0.5. It is found that when the solution to binder ration increased from 0.4 to 0.5, the spread diameter increased significantly. The spread diameter of alkaline paste reduced with the increase in the percentage of GGBFS as shown in Fig. 3. Dai et al. [47] studied slump flow of the pastes for 100% fly ash, 100% GGBFS,

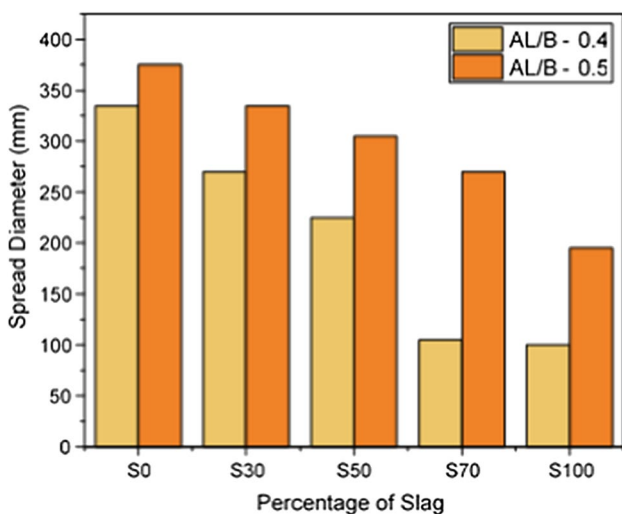


Fig. 3 Mini-slump spread diameter of alkali-activated pastes with different percentages of slag [38]

and 50% slag + 50% fly ash with varying alkaline liquid to binder ratio i.e. 0.27, 0.32, 0.37, and 0.42. Pangdaeng et al. [48] researched the flow test on Class C fly ash geopolymer with OPC as a partial replacement. The initial percentage of spread diameter of the pastes increased with an increase in alkaline to binder ratio for all three types of FA-GGBS based paste. the highest value of spread diameter was obtained by 50% GGBFS + 50% fly ash for 0.42 alkaline liquid to binder ratio. The flow of paste was halted around 30 min for 100% GGBFS pastes, while there was a constant flow of paste for 100% fly ash pastes because of the low reactivity of fly ash shown in Fig. 4. An addition of superplasticizers or extra water can be used to improve workability which may improve the applicability of alkali activated paste to various infrastructure projects [49]

Similar result was found in another study [50]. Kamath et al. [51] studied on fresh properties of alkali activated ternary paste with fly ash, GGBFS, and metakaolin binders. The slump flow value increased from 135 to 170 mm as the metakaolin percentage in the binder decreased from 20 to 5% due to the high surface area of metakaolin and its irregular form. Metakaolin is highly reactive in nature and reduces the flow significantly due to fast reactivity.

Setting time

Setting time is the essential property of fresh paste that defines the applicability especially in bulk concreting. The setting time varies with the influence of ratio of alkaline activator to binder, ratio of sodium silicate to sodium hydroxide, fly ash to slag ratio, and molarity of sodium hydroxide solution. Nath and Sarker [52] studied setting time on different fly ash to slag ratios with constant sodium silicate to sodium hydroxide ratio of 2.5, alkaline activator to binder ratio 0.4,

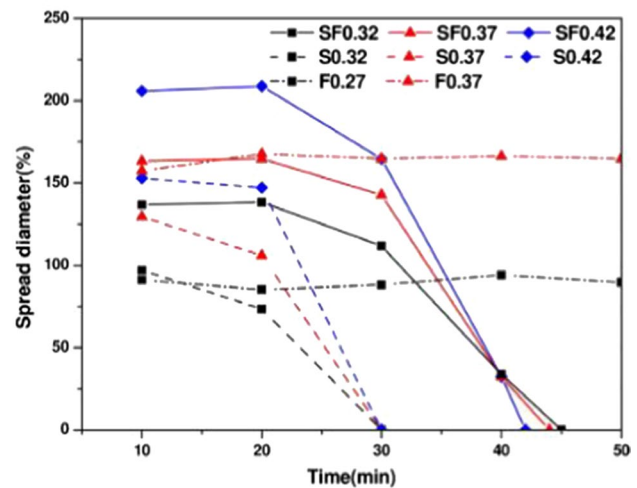


Fig. 4 Percentage of spread diameter with time [47]

and 14 M of NaOH. Fly ash was replaced with slag at 0%, 10%, 20%, and 30%. Fly ash with 100% content was used as the binder that reduces the initial setting time was more than 24 h which is because of slow polymerization. Addition of 10% slag was mixed with the fly ash than initial and final setting time was 290 min and 550 min. Further on increasing slag by 20% and 30% the setting decreased significantly as shown in Fig. 5). Slag was added into the alkali activated binders' mixture that reduce setting time with increase in slag content. Similar results were reported in other studies [26, 31, 35, 37, 53].

Fang et al. [54] investigated setting time on the alkaline liquid to binder ratio of 0.35 and 0.4 with varying slag replacement of 15%, 20%, and 25% respectively, ratio of sodium silicate to sodium hydroxide was 2, and molarity of sodium hydroxide was 10 M. The alkaline activator to binder ratio was increased from 0.35 to 0.4 than initial setting time was increased from 189 to 285 min for 15% slag replacement and 102 to 129 min for 25% slag replacement. The final setting time increased from 239 to 320 min for 15% slag replacement and 112 to 140 min for 25% slag replacement as illustrated in Fig. 6. As the alkaline activator to binder ratio reduces that shorter the set time due to the decrease in liquid content which resulting into accelerated reaction of binders. Similar findings were reported in other studies [26, 32]. with increase in Na_2SiO_3 to NaOH ratio, polymerization rate increases significantly, resulting into reduction of setting times [37]. [31, 32, 35]. t increase in molarity of NaOH resulted into reduction in setting time because of the increase in the hydroxide ion concentration [31, 35, 37] (Fig. 7). The effect of NaOH molarity on setting time is demonstrated in Fig. 8. Karim et al. [55] studied setting time without grinding and grinding of palm oil fuel ash and rice husk ash-based binders with different percentages of slag.

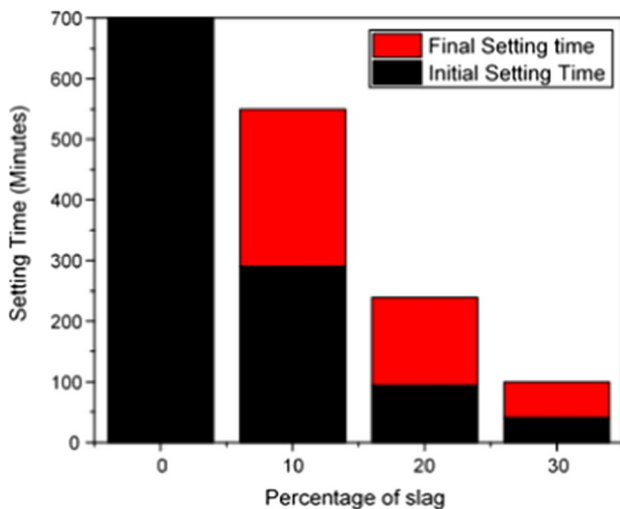


Fig. 5 Effect of different percentages of slag on setting time [52]

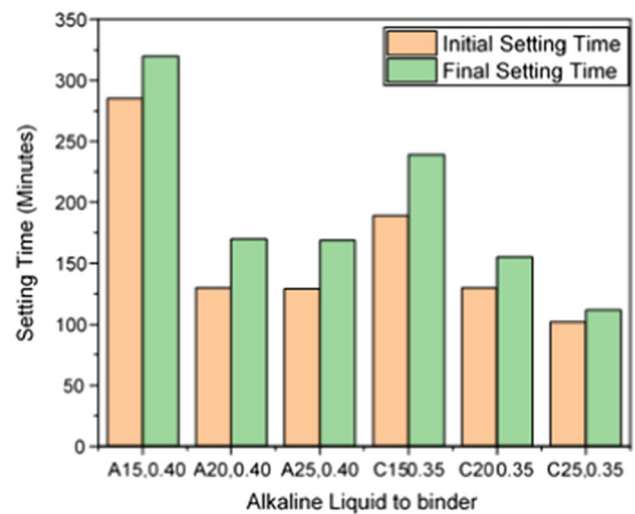


Fig. 6 Effect of Alkaline liquid to Binder ratio on setting time [54]

On reviewing recent literature, it is found that the binders which contain higher proportions of calcium results in lower setting times compared to low calcium binders. The setting also varies with the characteristics of liquid sodium silicate. Heating and curing conditions of alkali activated pastes also plays vital role in the reduction of setting time.

Mechanical properties of AAC

Compressive strength

Compressive strength (CS) is the mechanical property of concrete which enable the users to apply it to various

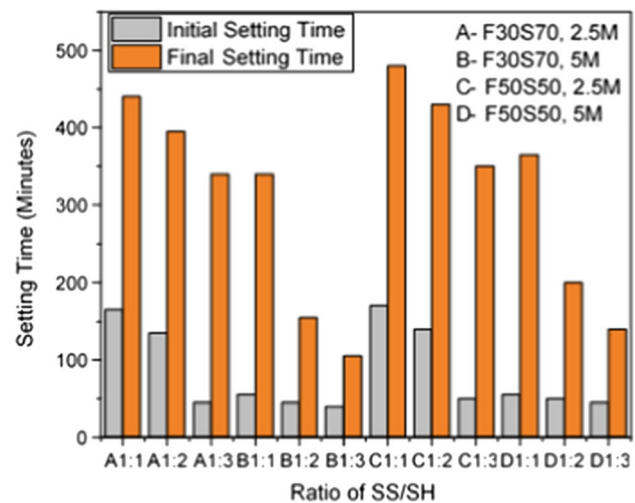


Fig. 7 Effect of Sodium Silicate to Sodium Hydroxide ratio on setting time [54]

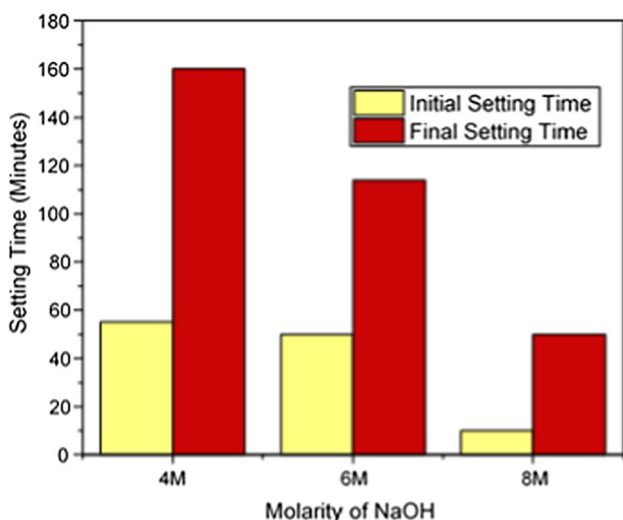


Fig. 8 Effect of Molarity of NaOH on setting time [82]

non- structural and structural application. The CS of AAC depends on parameters such as ratio of sodium silicate to sodium hydroxide, molarity of NaOH, alkaline activator to binder ratio, and curing regimes. Fernandez-Jimenez et al. [32] investigated on engineering properties of AAFSC. The CS of AAFSC increased rapidly in the first 24 h and slightly increased after 24 h. The CS of AASC increased from 17 to 66 MPa as the molarity of NaOH increased from 1 to 8 M [56]. As the molarity of sodium hydroxide increases polymerization process increases, while inducing sufficient alkalinity to the mix and enabling the dissolution of alumina and silica in the fly ash and GGBFS. [57] CS on different molarity of NaOH from 6 M, to 16 M with varying proportions of GGBFS in conjunction with fly ash has been studied. As the molarity of sodium hydroxide was increased from 6 to 16 M, the 28th-day compressive strength also increased from 18 to 32 MPa for 0% GGBFS and 45 MPa to 77 MPa for 50% GGBFS. (Fig. 9). Similar results were reported in other studies [27, 31, 35, 53, 58]. The early dissolution of aluminosilicate compounds with increasing molarity of NaOH above 16 M resulted in a decrease of CS. [58].

Nedeljkovic et al. [38] studied CS of AAC with two different ratios of the alkaline solution to the binder, i.e., 0.4 and 0.5. The alkaline liquid to binder ratio was increased that reduce CS slightly. Because of the decrease in consistency of mixes, the alkaline activation process of AAC decreases because of alkaline liquid to binder ratio decreases. Nath and Sarker [52] investigated on early strength properties of concrete with various alkaline liquid to binder ratios. The alkaline liquid to binder ratio was increased from 0.35 to 0.45, and the CS decreased gradually. The 28 strengths of concrete sample containing 10% GGBFS decreased by 24% for 0.40 ratio and 32% for 0.45 ratio compared to that of 0.35 ratio as illustrated in Fig. 10. Similar findings were reported in other

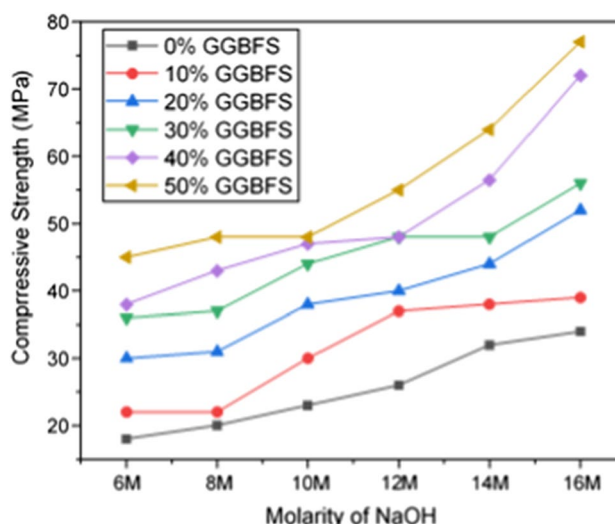


Fig. 9 Effect of different molarity of NaOH and percentage of GGBFS on compressive strength of concrete [57]

studies [31, 41]. Mehta et al. [14] conducted an experimental study on the mechanical properties of AAFSC. Fly ash was replaced with 0%, 5%, 10%, 15% and 20% of GGBFS as a binder. The early-age high strength values of AAC is due to polymerization reaction caused by aluminosilicate with the alkaline liquid, leading to the formation of N-A-S-H bonds. Similar observations were reported in other studies [53, 59].

Fang et al. [54] investigated on mechanical properties of AAFSC by varying the ratio of Na₂SiO₃ to NaOH. The CS of AAFSC specimens with a low Na₂SiO₃ to NaOH ratio was higher for higher curing age of the specimen increased than AAFSC specimens with a higher sodium silicate to sodium hydroxide ratio. Thomas and Peethamparan [60] studied on

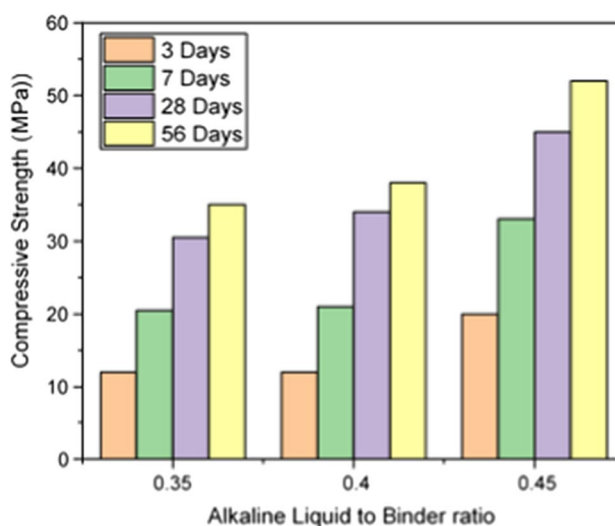


Fig. 10 Effect of Alkaline Liquid to Binder ratios on compressive strength of concrete [52]

engineering properties of AAC. The half of AAC samples were cured at 22 ± 1 °C for 28 ± 0.5 days (ambient temperature) with $> 95\%$ Relative Humidity, and the other half AAC specimens were cured at 50 ± 0.1 °C for 48 ± 0.25 h (elevated temperature). The ambient temperature cured AAC exhibits deficient compressive strength compared to higher temperature specimens. The compressive strength did not vary much when cured at ambient temperature and elevated temperature for alkali-activated slag concrete. [52]. Higher temperature causes excessive moisture loss and subsequent cracks in the specimen that may also result in strength loss [61]. Huseien et al. [62] studied on compressive strength of AAC with GGBFS and ceramic tile powder waste. The compressive strength decreased with an increase in the ceramic tile powder waste in the binders. The compressive strength value of the 56th day was similar in 0% and 10% ceramic tile powder waste replacing GGBFS. The compressive strength decreased from 70 to 30 MPa as the percentage of ceramic tile powder was increased from 0 to 80%. Mounika et al. [63] conducted experimental research on AAC using fly ash, GGBFS, and rice husk ash. The compressive strength of AAC using 90% fly ash and 10% rice husk ash increased from 7 to 34 MPa as the age of concrete from 3 to 28 days. The compressive strength of AAC using 90% GGBS and 10% rice husk ash increased from 26 to 59 MPa as the age of concrete from 3 to 28 days.

Split Tensile strength

Split Tensile strength is an important property of concrete because structural loads make it susceptible to tensile cracking. It is essential for a structural concrete to have sufficient Split tensile strength for defining its applicability in situations such as anchorage of reinforcing steel in concrete, initiation and propagation of cracks, and shear. The average splitting tensile strength (f_{st}) can be obtained by using ACI 318, 2008 [64] (Eq. (1)). Sofi et al. [65] also obtained the relationship between the CS and split tensile strength of AAC (Eq. (2)).

$$f_{st} = 0.56\sqrt{f_c'} \quad (1)$$

$$f_{st} = 0.48\sqrt{f_c'} \quad (2)$$

Wardhono et al. [66] compared the long-term properties of AASC and geopolymer concrete. The split tensile strength of AASC was found to be 3.3 MPa at 28 days and was constant till 540 days, whereas fly ash geopolymer concrete was 2.1 MPa at 28 days and increased to 4.1 MPa at 540 days shown in Fig. 11. The split tensile strength was greater when cured at ambient temperature than higher heat curing temperature [36, 67]. Fang et al. [54] studied on split tensile strength of AAFSC. The split tensile strength value

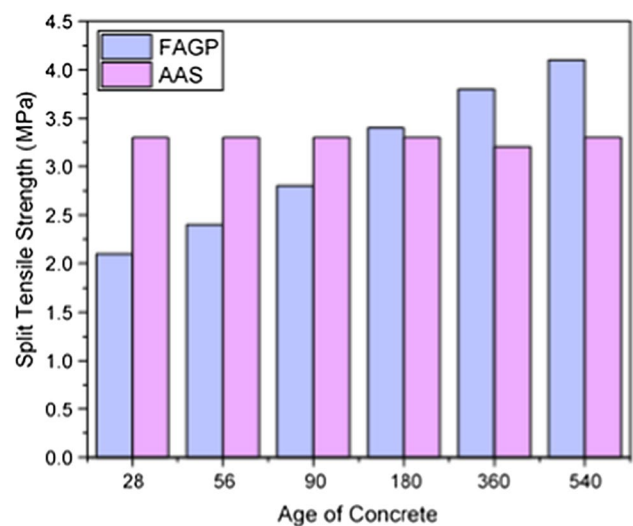


Fig. 11 Split Tensile Strength of AAS and FAGP vs. Age of concrete [66]

increased from 1.35 MPa to 3 MPa, when the percentage of slag was increased from 10 to 30%. Thunuguntla and Rao [56] investigated on mechanical and durability properties of AASC. The split tensile strength for concrete containing 1 M NaOH was 2.49 MPa, and it increased to 5.55 MPa with increase in the molarity of NaOH to 8 M. The split tensile strength increases as the fly ash content increase from 350 kg/m^3 to 400 kg/m^3 [68].

Flexural strength

The flexural strength yet another major mechanical property of concrete, representing the ability of the beam to resist failure due to bending. The flexural strength of OPC concrete, f_t is obtained using the ACI 318–08 [64] (Eq. (3)). Diaz-Loya et al. [69] also proposed the relationship between flexure strength and the compressive strength of AAC (Eq. (4)).

$$f_t = 0.62\sqrt{f_c'} \quad (3)$$

$$f_t = 0.69\sqrt{f_c'} \quad (4)$$

AASC developed higher flexure strength at an early age and gradually increased the strength over time [32]. Adak and Mandal [70] studied on mechanical properties of fly ash-based geopolymer concrete. The flexural strength of geopolymer concrete was prepared with the modified process, i.e., fly ash was mixed with the alkaline liquid and then heat-activated (60 °C) for 45 min before casting. Later, the geopolymer concrete specimen was placed at room temperature, giving higher strength than the geopolymer concrete that was heat-activated (60 °C at 48 h.) after casting.

Wardhono et al. [66] compared the engineering properties of AASC and geopolymer concrete. The flexural strength of geopolymer concrete increased gradually from 4.7 MPa at 28 days to 7.2 at 540 days while the strength decreased for AASC from 6 MPa at 28 days to 5.2 at 540 days. The flexural strengths of AAFSC in this study are slightly higher than PCC mixtures [60]. Parveen et al. [68] researched the flexural strength of the geopolymer concrete with varying quantities of binder material and the molarity of sodium hydroxide. The molarity of sodium hydroxide was increased from 8 to 16 M, and the tensile strength also increased from 3.43 to 4.23 for content of 400 kg/m³ fly ash. Fly ash content increased from 350 to 400 kg/m³; tensile strength increased from 3 to 6%, as shown in Fig. 12. A similar result was also found in another study [56].

Durability properties of AAC

Durability of concrete provides the information about the long-term performance which is one of essential parameter to comment on applicability to long term performance of structural concrete. The preliminary factors able to measure the long term properties of AAC concrete and AAC mortar indicate an excellent quality of concrete with thermal resistance, heat of hydration, water absorption and permeability, porosity, corrosion resistance, alkali-silica reaction and sulphates, chloride attack.

Water absorption and water permeability

Water absorption and water permeability is such a parameter which shows the transport way of water but also provide water resistance capacity of alkali activated binders

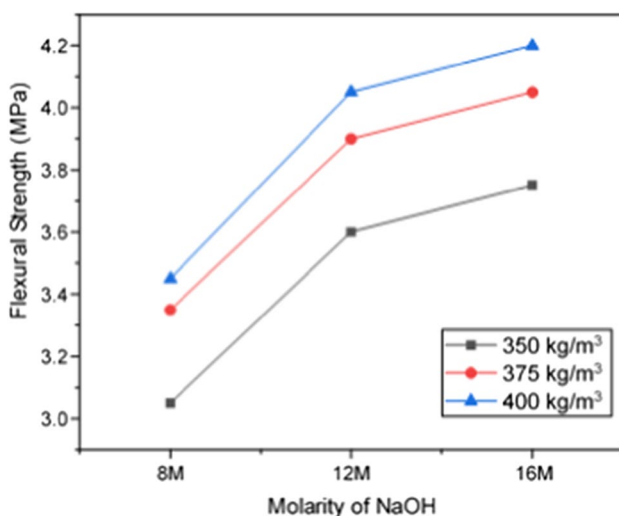


Fig. 12 Effect of Molarity of NaOH on Flexural strength[68]

and concretes. Researchers studied the influence of liquid alkali activator and use of silica fume (SF) on durability and microstructural properties of AASC pastes [49, 71–75]. The linear regression of porosity versus compressive is shown in Fig. 13a and b, which shows direct relationship between both the properties. Also, relationship of electrical resistivity versus compressive is shown in Fig. 13c and d. With the use of recycled aggregates [57] higher concentrations activators is required to have similar durability characteristics. In several alkali activated concretes, similar outcomes have been observed [44, 55, 57].

Acid attacks

The acid attacks is the main characteristics properties of durability studies which highlight the performance of concrete in sever environment. Kirubajiny et al. (2017) have reported the durability aspects of (FGPC) culvert was casted that exposed to coastal environment for 6 years. The effect of carbonation was observed in fly-ash-based-geo-polymer concrete (FGPC) for 6 years. FGPC culvert was carbonated in the top slab 135 mm and leg 90 mm while OPC culvert shown maximum value of 10 mm and 20 mm respectively. Chloride resistance in the FGPC was high (2.5 times) when compared to OPC in the coastal environment. Microstructural test results confirmed that the dissolutions of carbonation in FGPC when exposed to the actual conditions, whereas leaching was detected in the normal concrete. Also, SEM/EDX images showed that the chloride was precipitated as a layer on the FGPC. Simultaneously, from images was observed that the higher sulfate penetration and no development of C-A-S-H in the FGPC. Even though geo-polymer-concrete the amount of porosity was better than conventional concrete, the area of the pore was fined pores stuck between 1.25 and 25 nm diameter, while the near all the pores in ordinary concrete in the range of 25 nm to 50,000 nm. Some other investigation based on a similar finding [76–78].

Albitar et al. (2017) studied the long-term performance of geo-polymer and traditional concrete. In this study, the geo-polymer concrete was produced using either fly-ash or blended slag and fly-ash. Concrete cube was constantly kept up to 9 months in 4 chemical solutions: 5% NaCl, 5% Na₂SO₄, 5% MgSO₄ and 3% H₂SO₄. OPC concrete was found to have lower sorptivity and water absorption rate in comparison with slag (GLSS) and fly-ash based geo-polymer concrete. Normal concrete (OPC) suffered higher deterioration than geo-polymer concrete due to sodium sulfate environment with reduction of volume by 15% compared to 13% and 12% of slag and fly-ash based geopolymer concrete respectively. H₂SO₄ (Sulfuric acid) has an additional disadvantageous impact on normal concrete (OPC) with a decrease in strength (compressive) of 26% compared to 10% and 7% reduction of fly-ash and slag (GLSS) geo-polymer

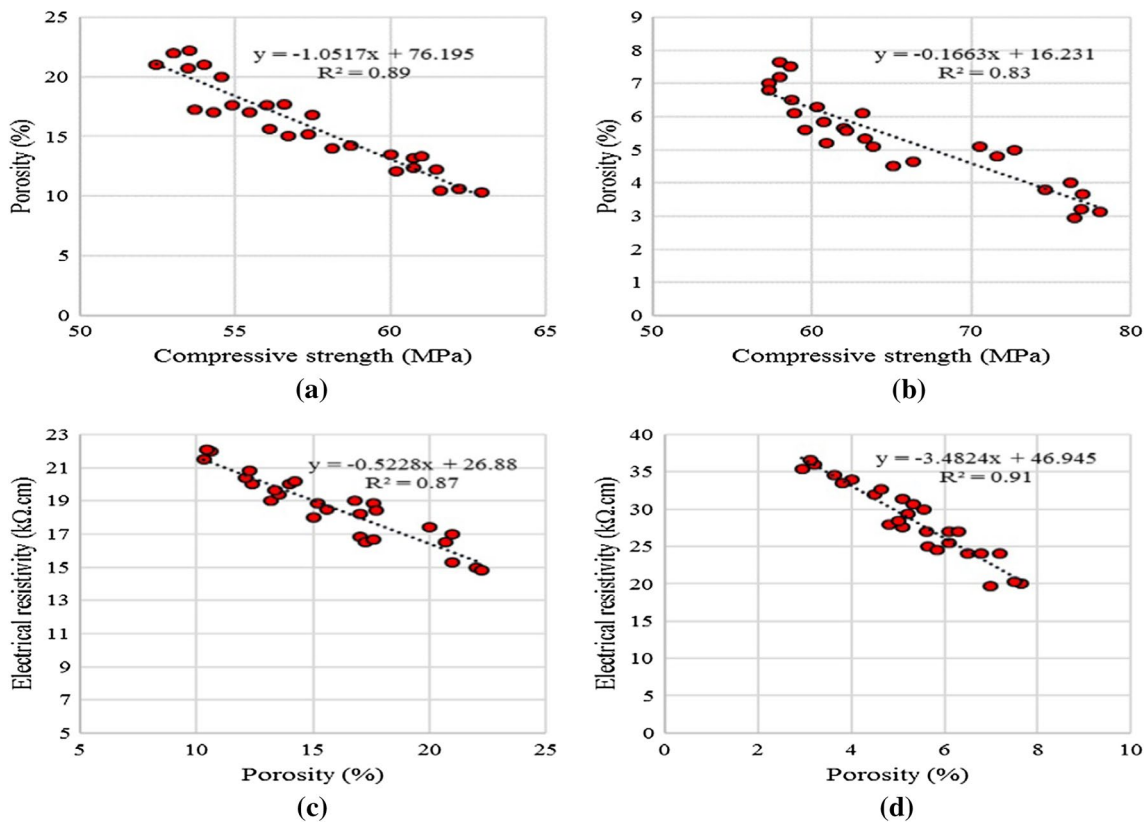


Fig. 13 a and b Relationship between Porosity and Compressive strength c and d Relationship between Electrical Resistivity and Compressive strength

concrete respectively. Geo-polymer concrete showed the better long term durability when exposed to chemical attack compared to OPC based concrete [79].

Mahdi et al. (2019) studied the compressive strength and long-term performance of recycled aggregate concrete with various proportion of SS and SH. Change in the SS/SH proportion from 2 to 3 increased the compressive strength of up to 6%. Micrograph images of the interfacial state between aggregate and geo-polymer paste with no re-cycled aggregate concrete specimen showed denser and compacted matrix comparing to re-cycled aggregate geo-polymer concrete. Geo-polymer gel with re-cycled aggregate was found to have higher porosity at the interstate paste and re-cycled aggregate. Moreover, additional geo-polymerization compounds including C–A–S–H, N–A–S–H or C–S–H and mono/tri sulfate with the needle was found in the matrix structure [80]. From the Fig. 14 the relationship between electrical resistivity and RPCT with compressive has been studied.

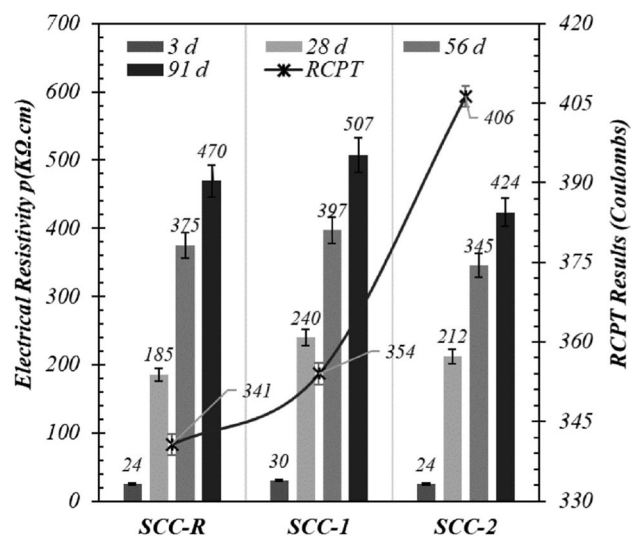


Fig. 14 Electrical resistivity and chloride penetrability versus Compressive strength

Conclusion

Based on the available literature on materials used for manufacturing AAC, fresh properties of AAB, and the mechanical properties of AAC, the following general conclusions are drawn:

- Major industrial by-products used to manufacture AAC are fly ash (Class F) and GGBFS due to their high aluminosilicate and calcium content. Since they are readily available, slight modification and careful selection of activator concentration can enhance the applicability of AAMs for general purpose concreting.
- The molarity of NaOH and the ratio of Na_2SiO_3 to NaOH impacts the setting time and flow properties of paste of AAB due to changes in the viscosity as the dissolution of aluminosilicates in the alkaline solution proceeds.
- Influence of activator concentration, influence of additives on flyash/slag based AAMs and their collective influence on mechanical and durability aspects of concrete signifies AAM as potential binder for general construction purpose.
- Setting time and consistency has to be further researched by conducting detailed study on reaction mechanism with various additives can increase the applicability of AAMs.
- The challenges involved in AAM is the long-term performance is remaining an unexplored area with many industrial and agro based binders. This will promote use of local materials and move another step towards development of eco-friendly concrete. The thermodynamic, chemical stability and rheology study of AAM another aspect which is not addressed still.
- High Performance AAM binders are not researched which will provide construction industry to apply for new generation structures and will prove to be a low carbon alternative to conventional concrete.

Funding No external funding was used.

Declarations

Conflict of interest The authors declare that they have no conflict of interest.

Open Access This article is licensed under a Creative Commons Attribution 4.0 International License, which permits use, sharing, adaptation, distribution and reproduction in any medium or format, as long as you give appropriate credit to the original author(s) and the source, provide a link to the Creative Commons licence, and indicate if changes were made. The images or other third party material in this article are included in the article's Creative Commons licence, unless indicated otherwise in a credit line to the material. If material is not included in the article's Creative Commons licence and your intended use is not permitted by statutory regulation or exceeds the permitted use, you will

need to obtain permission directly from the copyright holder. To view a copy of this licence, visit <http://creativecommons.org/licenses/by/4.0/>.

References

1. Mehta PK (2001) Reducing the Environmental Impact of Concrete. *Concr Int* 23(10):61–66
2. Kumar M, Shreelaxmi P, Kamath M (2021) Review on characteristics of sewage sludge ash and its partial replacement as binder material in concrete, pp. 65–78
3. Chippagiri R, Gavali HR, Ralegaonkar RV, Riley M, Shaw A, Bras A (2021) Application of sustainable prefabricated wall technology for energy efficient social housing. *Sustain* 13(3):1–12. <https://doi.org/10.3390/su13031195>
4. Scharff H (2014) Landfill reduction experience in The Netherlands. *Waste Manag* 34(11):2218–2224. <https://doi.org/10.1016/j.wasman.2014.05.019>
5. Sikora P et al (2021) The effects of nano- and micro-sized additives on 3D printable cementitious and alkali-activated composites: a review. *Appl Nanosci*. <https://doi.org/10.1007/s13204-021-01738-2>
6. Sotelo-Piña C, Aguilera-González EN, Martínez-Luévanos A (2019) Geopolymers: Past, present, and future of low carbon footprint eco-materials. *Handb Ecomater* 4:2765–2785. https://doi.org/10.1007/978-3-319-68255-6_54
7. Yousuf A, Manzoor SO, Youssouf M, Malik ZA, Sajjad Khawaja K (2020) Fly Ash: Production and Utilization in India-An Overview. *J Mater Environ Sci* 2020(6):911–921
8. Mehta A, Siddique R (2016) An overview of geopolymers derived from industrial by-products. *Constr Build Mater*. <https://doi.org/10.1016/j.conbuildmat.2016.09.136>
9. Athira VS, Charitha V, Athira G, Bahurudeen A (2021) Agro-waste ash based alkali-activated binder: Cleaner production of zero cement concrete for construction. *J Clean Prod* 286:125429. <https://doi.org/10.1016/j.jclepro.2020.125429>
10. Yang K-H, Song J-K, Song K-I (2013) Assessment of CO₂ reduction of alkali-activated concrete. *J Clean Prod* 39:265–272. <https://doi.org/10.1016/j.jclepro.2012.08.001>
11. Ruiz-Santaquiteria C, Fernández-Jiménez A, Palomo A (2016) Alternative prime materials for developing new cements: Alkaline activation of alkali aluminosilicate glasses. *Ceram Int* 42(8):9333–9340. <https://doi.org/10.1016/j.ceramint.2016.03.111>
12. Ng C, Alengaram UJ, Wong LS, Mo KH, Jumaat MZ, Ramesh S (2018) A review on microstructural study and compressive strength of geopolymer mortar, paste and concrete. *Constr Build Mater* 186:550–576. <https://doi.org/10.1016/j.conbuildmat.2018.07.075>
13. Ibrahim M, Maslehuddin M (2021) An overview of factors influencing the properties of alkali-activated binders. *J Clean Prod* 286:124972. <https://doi.org/10.1016/j.jclepro.2020.124972>
14. Mehta A, Siddique R, Ozbakkaloglu T, Shaikh FUA, Belarbi R (2020) Fly ash and ground granulated blast furnace slag-based alkali-activated concrete: Mechanical, transport and microstructural properties". *Constr Build Mater* 257:119548. <https://doi.org/10.1016/j.conbuildmat.2020.119548>
15. Opiso EM, Tabelin CB, Maestre CV, Aseniero JPI, Villacorte-Tabelin M (2021) Synthesis and characterization of coal fly ash and palm oil fuel ash modified artisanal and small-scale gold mine (ASGM) tailings based geopolymer using sugar mill lime sludge as Ca-based activator. *Heliyon* 7(4):e06654. <https://doi.org/10.1016/j.heliyon.2021.e06654>

16. Shalini A, Gurunarayanan G, Kumar R, Prakash V, Sakthivel S (2016) Performance of Rice Husk Ash in Geopolymer Concrete. *Int J Innov Res Sci Technol* 2(12):73–77
17. Kamath MV, Prashanth S, Kumar M (2021) Review of Low to High Strength Alkali-Activated and Geopolymer Concrete, 105
18. Hossain MM et al (2020) Water absorption and sorptivity of alkali-activated ternary blended composite binder. *J Build Eng* 31(Augus 2019):101370. <https://doi.org/10.1016/j.jobe.2020.101690>
19. Manjunath R, Narasimhan MC (2018) An experimental investigation on self-compacting alkali activated slag concrete mixes. *J Build Eng* 17(January):1–12. <https://doi.org/10.1016/j.jobe.2018.01.009>
20. Duxson P, Provis JL, Lukey GC, van Deventer JSJ (2007) The role of inorganic polymer technology in the development of 'green concrete.' *Cem Concr Res* 37(12):1590–1597. <https://doi.org/10.1016/j.cemconres.2007.08.018>
21. Moro C, Francioso V, Velay-Lizancos M (2021) Modification of CO₂ capture and pore structure of hardened cement paste made with nano-TiO₂ addition: Influence of water-to-cement ratio and CO₂ exposure age. *Constr Build Mater* 275:122131. <https://doi.org/10.1016/j.conbuildmat.2020.122131>
22. Kalombe RM, Ojumu VT, Eze CP, Nyale SM, Kevern J, Petrik LF (2020) Fly ash-based geopolymer building materials for green and sustainable development. *Materials (Basel)* 13(24):1–17. <https://doi.org/10.3390/ma13245699>
23. H. Kuhl, "Slag Cement and Process of Making the Same," 900,939, 1908.
24. Chassevent L (1937) Hydraulicity of slags. *Compt Rend* 205:670–672
25. Purdon A (1940) The action of alkalis on blast-furnace slag. *J Soc Chem Ind* 59:191–202
26. Glukhovskiy VD (1959) "Soil Silicates. Kiev," *USSR Gostroiizdat*
27. Davidovits J (1979) Synthesis of new high-temperature geopolymers for reinforced plastics/composites., in *Spe pactec*, pp. 151–154
28. Davidovits J, Sawyer JL (1985) "Early high-strength mineral polymer," 4,509,985
29. Douglas E, Bilodeau A, Brandstetr J, Malhotra VM (1991) Alkali activated ground granulated blast-furnace slag concrete: Preliminary investigation. *Cem Concr Res* 21(1):101–108. [https://doi.org/10.1016/0008-8846\(91\)90036-H](https://doi.org/10.1016/0008-8846(91)90036-H)
30. Wang SD, Scrivener KL (1995) Hydration products of alkali activated slag cement. *Cem Concr Res* 25(3):561–571. [https://doi.org/10.1016/0008-8846\(95\)00045-E](https://doi.org/10.1016/0008-8846(95)00045-E)
31. Palomo A, Grutzeck MW, Blanco MT (1999) Alkali-activated fly ashes. *Cem Concr Res* 29(8):1323–1329. [https://doi.org/10.1016/S0008-8846\(98\)00243-9](https://doi.org/10.1016/S0008-8846(98)00243-9)
32. Fernández-Jiménez AM, Palomo A, López-Hombrados C (2006) Engineering Properties of Alkali-Activated Fly Ash Concrete. *ACI Mater J* 103(2):106–112. <https://doi.org/10.14359/15261>
33. Aperador W, Mejía de Gutiérrez R, Bastidas DM (2009) Steel corrosion behaviour in carbonated alkali-activated slag concrete. *Corros Sci* 51(9):2027–2033. <https://doi.org/10.1016/j.corosci.2009.05.033>
34. Chi M (2012) Effects of dosage of alkali-activated solution and curing conditions on the properties and durability of alkali-activated slag concrete. *Constr Build Mater* 35:240–245. <https://doi.org/10.1016/j.conbuildmat.2012.04.005>
35. Gomaa E, Han T, ElGawady M, Huang J, Kumar A (2021) Machine learning to predict properties of fresh and hardened alkali-activated concrete. *Cem Concr Compos* 115(May 2020):103863. <https://doi.org/10.1016/j.cemconcomp.2020.103863>
36. Elahi MMA, Hossain MM, Karim MR, Zain MFM, Shearer C (2020) A review on alkali-activated binders: Materials composition and fresh properties of concrete. *Constr Build Mater* 260:119788. <https://doi.org/10.1016/j.conbuildmat.2020.119788>
37. ASTM C618-12a (2014) *Standard Specification for Coal Fly Ash and Raw or Calcined Natural Pozzolan for Use in Concrete.*, pp 1–5
38. Nedeljković M, Li Z, Ye G (2018) Setting, strength, and Autogenous shrinkage of alkali-activated fly ash and slag pastes: effect of slag content. *Materials (Basel)* 11(11):2121. <https://doi.org/10.3390/ma11112121>
39. Topark-Ngarm P, Chindaprasirt P, Sata V (2015) Setting Time, Strength, and Bond of High-Calcium Fly Ash Geopolymer Concrete. *J Mater Civ Eng*. [https://doi.org/10.1061/\(asce\)jmt.1943-5533.0001157](https://doi.org/10.1061/(asce)jmt.1943-5533.0001157)
40. Duxson P (2009) Geopolymer precursor design. In: *Geopolymers*, Elsevier, pp. 37–49
41. Tantri A, Nayak G, Shenoy A, Shetty KK (2021) Development of self-compacting concrete using Bailey aggregate grading technique in comparison with Indian standard code of practice. *J Eng Des Technol*. <https://doi.org/10.1108/JEDT-02-2021-0095>
42. Balamuralikrishnan R, Saravanan J (2021) Effect of addition of alccofine on the compressive strength of cement mortar cubes. *Emerg Sci J* 5(2):155–170. <https://doi.org/10.28991/esj-2021-01265>
43. Davidovits J (1991) Geopolymers: Inorganic polymeric new materials. *J Therm Anal* 37(8):1633–1656. <https://doi.org/10.1007/BF01912193>
44. Amer I, Kohail M, El-Feky MS, Rashad A, Khalaf MA (2021) A review on alkali-activated slag concrete. *Ain Shams Eng J*. <https://doi.org/10.1016/j.asej.2020.12.003>
45. Jiao Z, Wang Y, Zheng W, Huang W (2018) Effect of dosage of sodium carbonate on the strength and drying shrinkage of sodium hydroxide based alkali-activated slag paste. *Constr Build Mater* 179:11–24. <https://doi.org/10.1016/j.conbuildmat.2018.05.194>
46. ASTM C 1437-07 (2007) Standard Test Method for Flow of Hydraulic Cement Mortar, *ASTM Int.*, pp. 6–7
47. Dai X, Aydin S, Yardimci MY, Lesage K, de Schutter G (2020) Influence of water to binder ratio on the rheology and structural Build-up of Alkali-Activated Slag/Fly ash mixtures. *Constr Build Mater* 264:120253. <https://doi.org/10.1016/j.conbuildmat.2020.120253>
48. Pangdaeng S, Phoo-ngernkham T, Sata V, Chindaprasirt P (2014) Influence of curing conditions on properties of high calcium fly ash geopolymer containing Portland cement as additive. *Mater Des* 53:269–274. <https://doi.org/10.1016/j.matdes.2013.07.018>
49. Chindaprasirt P, Chareerat T, Sirivivatnanon V (2007) Workability and strength of coarse high calcium fly ash geopolymer. *Cem Concr Compos* 29(3):224–229. <https://doi.org/10.1016/j.cemconcomp.2006.11.002>
50. Nematollahi B, Sanjayan J (2014) Effect of different superplasticizers and activator combinations on workability and strength of fly ash based geopolymer. *Mater Des* 57:667–672. <https://doi.org/10.1016/j.matdes.2014.01.064>
51. Kamath M, Prashant S, Kumar M (2021) Micro-characterisation of alkali activated paste with fly ash-GGBS-metakaolin binder system with ambient setting characteristics. *Constr Build Mater*. <https://doi.org/10.1016/j.conbuildmat.2021.122323>
52. Nath P, Sarker PK (2014) Effect of GGBFS on setting, workability and early strength properties of fly ash geopolymer concrete cured in ambient condition. *Constr Build Mater* 66:163–171. <https://doi.org/10.1016/j.conbuildmat.2014.05.080>
53. Dineshkumar M, Umarani C (2020) Effect of Alkali Activator on the Standard Consistency and Setting Times of Fly Ash and GGBS-Based Sustainable Geopolymer Pastes. *Adv Civ Eng* 2020:1–10. <https://doi.org/10.1155/2020/2593207>

54. Fang G, Ho WK, Tu W, Zhang M (2018) Workability and mechanical properties of alkali-activated fly ash-slag concrete cured at ambient temperature. *Constr Build Mater* 172:476–487. <https://doi.org/10.1016/j.conbuildmat.2018.04.008>
55. Karim MR, Zain MFM, Jamil M, Lai FC (2013) Fabrication of a non-cement binder using slag, palm oil fuel ash and rice husk ash with sodium hydroxide. *Constr Build Mater* 49:894–902. <https://doi.org/10.1016/j.conbuildmat.2013.08.077>
56. Thunuguntla CS, Gunneswara Rao TD (2018) Effect of mix design parameters on mechanical and durability properties of alkali activated slag concrete. *Constr Build Mater* 193:173–188. <https://doi.org/10.1016/j.conbuildmat.2018.10.189>
57. Saha S, Rajasekaran C (2017) Enhancement of the properties of fly ash based geopolymer paste by incorporating ground granulated blast furnace slag. *Constr Build Mater* 146:615–620. <https://doi.org/10.1016/j.conbuildmat.2017.04.139>
58. Somna K, Jaturapitakkul C, Kajitvichyanukul P, Chindaprasirt P (2011) NaOH-activated ground fly ash geopolymer cured at ambient temperature. *Fuel* 90(6):2118–2124. <https://doi.org/10.1016/j.fuel.2011.01.018>
59. Sarker PK (2011) Bond strength of reinforcing steel embedded in fly ash-based geopolymer concrete. *Mater Struct* 44(5):1021–1030. <https://doi.org/10.1617/s11527-010-9683-8>
60. Thomas RJ, Peethamparan S (2015) Alkali-activated concrete: Engineering properties and stress–strain behavior. *Constr Build Mater* 93:49–56. <https://doi.org/10.1016/j.conbuildmat.2015.04.039>
61. Okoye FN, Durgaprasad J, Singh NB (2015) Mechanical properties of alkali activated flyash/Kaolin based geopolymer concrete. *Constr Build Mater* 98:685–691. <https://doi.org/10.1016/j.conbuildmat.2015.08.009>
62. Huseien GF, Sam ARM, Shah KW, Mirza J (2020) Effects of ceramic tile powder waste on properties of self-compacted alkali-activated concrete. *Constr Build Mater* 236:117574. <https://doi.org/10.1016/j.conbuildmat.2019.117574>
63. Mounika G, Ramesh B, Kalyana Rama JS (2020) Experimental investigation on physical and mechanical properties of alkali activated concrete using industrial and agro waste. *Mater Today Proc* 33:4372–4376. <https://doi.org/10.1016/j.matpr.2020.07.634>
64. ACI Committee (2008) Building Code Requirements for Structural Concrete (ACI 318–08) and Commentary. *Am Concr Inst*
65. Sofi M, van Deventer JSJ, Mendis PA, Lukey GC (2007) Engineering properties of inorganic polymer concretes (IPCs). *Cem Concr Res* 37(2):251–257. <https://doi.org/10.1016/j.cemconres.2006.10.008>
66. Wardhono A, Gunasekara C, Law DW, Setunge S (2017) Comparison of long term performance between alkali activated slag and fly ash geopolymer concretes. *Constr Build Mater*. <https://doi.org/10.1016/j.conbuildmat.2017.03.153>
67. Sarker PK, Haque R, Ramgolam KV (2013) Fracture behaviour of heat cured fly ash based geopolymer concrete. *Mater Des* 44:580–586. <https://doi.org/10.1016/j.matdes.2012.08.005>
68. Parveen DS, Junaid MT, Jindal BB, Mehta A (2018) Mechanical and microstructural properties of fly ash based geopolymer concrete incorporating alccofine at ambient curing. *Constr Build Mater* 180(2018):298–307. <https://doi.org/10.1016/j.conbuildmat.2018.05.286>
69. Diaz-Loya EI, Allouche EN, Vaidya S (2011) Mechanical properties of fly-ash-based geopolymer concrete. *ACI Mater J* 108(3):300–306. <https://doi.org/10.14359/51682495>
70. Adak D, Mandal S (2019) Strength and Durability Performance of Fly Ash-Based Process-Modified Geopolymer Concrete. *J Mater Civ Eng* 31(9):04019174. [https://doi.org/10.1061/\(ASCE\)MT.1943-5533.0002793](https://doi.org/10.1061/(ASCE)MT.1943-5533.0002793)
71. Shariati M et al (2020) Alkali-activated slag (AAS) paste: Correlation between durability and microstructural characteristics. *Constr Build Mater*. <https://doi.org/10.1016/j.conbuildmat.2020.120886>
72. Gavali HR, Ralegaonkar RV (2020) Design of eco-efficient housing with sustainable alkali-activated bricks. *J Clean Prod*. <https://doi.org/10.1016/j.jclepro.2020.120061>
73. Majhi RK, Nayak AN, Mukharjee BB (2018) Development of sustainable concrete using recycled coarse aggregate and ground granulated blast furnace slag. *Constr Build Mater* 159:417–430. <https://doi.org/10.1016/j.conbuildmat.2017.10.118>
74. Jagadisha A, Rao KB, Nayak G, Kamath M (2021) Influence of nano-silica on the microstructural and mechanical properties of high-performance concrete of containing EAF aggregate and processed quarry dust. *Constr Build Mater* 304:124392. <https://doi.org/10.1016/j.conbuildmat.2021.124392>
75. Elzokra A, Al Hourri A, Habib A, Habib M, Malkawi AB (2020) Shrinkage behavior of conventional and nonconventional concrete: A review. *Civ Eng J* 6(9):1839–1851. <https://doi.org/10.28991/cej-2020-03091586>
76. Zhang ZH, Zhu HJ, Zhou CH, Wang H (2016) Geopolymer from kaolin in China: An overview. *Appl Clay Sci* 119:31–41. <https://doi.org/10.1016/j.clay.2015.04.023>
77. Ye H, Chen Z, Huang L (2019) Mechanism of sulfate attack on alkali-activated slag: the role of activator composition. *Cem Concr Res* 125(August):105868. <https://doi.org/10.1016/j.cemconres.2019.105868>
78. Awoyera P, Adesina A (2019) A critical review on application of alkali activated slag as a sustainable composite binder. *Case Stud Constr Mater* 11:e00268. <https://doi.org/10.1016/j.cscm.2019.e00268>
79. Albitar M, Mohamed Ali MS, Visintin P, Drechsler M (2017) Durability evaluation of geopolymer and conventional concretes. *Constr Build Mater* 136:374–385. <https://doi.org/10.1016/j.conbuildmat.2017.01.056>
80. Safhi A el M, Rivard P, Yahia A, Henri Khayat K, Abriak NE (2021) Durability and transport properties of SCC incorporating dredged sediments. *Constr Build Mater*, 288:123116, <https://doi.org/10.1016/j.conbuildmat.2021.123116>
81. Mendes BC et al (2020) Application of eco-friendly alternative activators in alkali-activated materials: A review. *J Build Eng* 35(November):2021. <https://doi.org/10.1016/j.jobbe.2020.102010>
82. Lee NK, Lee HK (2013) Setting and mechanical properties of alkali-activated fly ash/slag concrete manufactured at room temperature. *Constr Build Mater* 47:1201–1209. <https://doi.org/10.1016/j.conbuildmat.2013.05.107>
83. Stolz J, Boluk Y, Bindiganavile V (2018) Mechanical, thermal and acoustic properties of cellular alkali activated fly ash concrete. *Cem Concr Compos* 94(June):24–32. <https://doi.org/10.1016/j.cemconcomp.2018.08.004>
84. Adak D, Sarkar M, Mandal S (2017) Structural performance of nano-silica modified fly-ash based geopolymer concrete. *Constr Build Mater* 135:430–439. <https://doi.org/10.1016/j.conbuildmat.2016.12.111>
85. Mohankumar G, Manickavasagam R (2017) Study on the development of class C flyash based GPC by ambient curing. *Int J Appl Eng Res* 12(7):1227–1231
86. Duan P, Yan C, Zhou W (2017) Compressive strength and microstructure of fly ash based geopolymer blended with silica fume under thermal cycle. *Cem Concr Compos* 78:108–119. <https://doi.org/10.1016/j.cemconcomp.2017.01.009>
87. Sakulich AR, Anderson E, Schauer C, Barsoum MW (2009) Mechanical and microstructural characterization of an alkali-activated slag/limestone fine aggregate concrete. *Constr Build*

- Mater 23(8):2951–2957. <https://doi.org/10.1016/j.conbuildmat.2009.02.022>
88. Sevinç AH, Durgun MY (2020) Properties of high-calcium fly ash-based geopolymer concretes improved with high-silica sources. *Constr Build Mater* 261:120014. <https://doi.org/10.1016/j.conbuildmat.2020.120014>
 89. Das SK et al (2020) Fresh, strength and microstructure properties of geopolymer concrete incorporating lime and silica fume as replacement of fly ash. *J Build Eng* 32:101780. <https://doi.org/10.1016/j.jobe.2020.101780>
 90. Khan MZN, Shaikh FUA, Hao Y, Hao H (2016) Synthesis of high strength ambient cured geopolymer composite by using low calcium fly ash. *Constr Build Mater* 125:809–820. <https://doi.org/10.1016/j.conbuildmat.2016.08.097>
 91. Bicer A (2018) Effect of fly ash particle size on thermal and mechanical properties of fly ash-cement composites. *Therm Sci Eng Prog* 8(July):78–82. <https://doi.org/10.1016/j.tsep.2018.07.014>
 92. Agrawal US, Wanjari SP, Naresh DN (2017) Characteristic study of geopolymer fly ash sand as a replacement to natural river sand. *Constr Build Mater* 150:681–688. <https://doi.org/10.1016/j.conbuildmat.2017.06.029>